ARCHIVES OF BIOCHEMISTRY AND BIOPHYSICS
Vol. 329, No. 1, May 1, pp. 56–64, 1996
Article No. 0191

# Characterization of Products from the Reactions of *N*-Acetyldopamine Quinone with *N*-Acetylhistidine

Rongda Xu,* Xin Huang,* Thomas D. Morgan,† Om Prakash,‡
Karl J. Kramer,†‡,[1] and M. Dale Hawley*

*Departments of *Chemistry and ‡Biochemistry, Kansas State University, Manhattan, Kansas 66506; and †U.S. Grain Marketing Research Laboratory, Agricultural Research Service, United States Department of Agriculture,*[2] Manhattan, Kansas 66502

Received December 18, 1995, and in revised form February 12, 1996

When insects harden or sclerotize their exoskeletons, quinones of *N*-acetylated catecholamines such as *N*-acetyldopamine (NADA) undergo nucleophilic addition reactions with amino acids such as histidine in cuticular proteins. To determine the products that might form when this type of reaction occurs during cuticle sclerotization, the reactions between electrochemically prepared NADA quinone and *N*-acetylhistidine (NAcH), a protein model nucleophile, have been investigated at pH 7. Two major products, 6-[*N*-(*N*-acetylhistidyl)]-*N*-acetyldopamine and 2-[*N*-(*N*-acetylhistidyl)]-*N*-acetyldopamine, were purified by semipreparative reversed-phase liquid chromatography and identified by mass spectrometry and nuclear magnetic resonance spectroscopy. The relative molar ratio of the C(6) mono-addition adduct to the C(2) mono-addition adduct is 87:13. UV/vis spectroscopic analysis shows that both products have an absorption maximum at 284 nm. Cyclic voltammetry shows that these adducts are oxidized less readily than NADA. 

*Key Words:* quinone; catecholamine; cuticle; histidine; protein; sclerotization; adduct; oxidation; addition.

*N*-Acylcatecholamines are important catecholamine metabolites used by insects to sclerotize or harden their exoskeletons. *N*-Acetyldopamine (NADA)[3] and *N*-$\beta$-alanyldopamine are oxidized to quinones that undergo nucleophilic addition by amino acid side chains in cuticular proteins (1–3). Covalent bonds that are formed between the aromatic ring of NADA and cuticular protein amino acids, such as histidine and lysine, have been detected in insect cuticle using solid-state double cross polarization $^{13}C$ and $^{15}N$ NMR (4). Cross-links between the $\beta$-carbon (C7) in the side chain of dopamine derivatives and histidine residues have been found in cuticle by rotational echo double resonance NMR (5). Catecholamine-containing proteins have been isolated from insect cuticle undergoing sclerotization (6). Cuticle-catalyzed coupling between NADA and *N*-acetylhistidine (NAcH) has been studied *in vitro,* and both $\beta$- and ring C6-addition adducts have been detected (2).

The goal of this study was to determine the initial steps of the oxidation reaction pathway of NADA when a nucleophile is present in excess. To mimic the cuticle-catalyzed reactions, we investigated a model system for cuticle sclerotization in which electrochemically prepared NADA quinone was reacted with a typical protein nucleophile, NAcH. Reactions were studied using reversed-phase liquid chromatography (LC), cyclic voltammetry (CV), and UV/vis spectroscopy. The two major products, 6-[*N*-(*N*-acetylhistidyl)]-*N*-acetyldopamine and 2-[*N*-(*N*-acetylhistidyl)]-*N*-acetyldopamine, were characterized by fast atom bombardment mass spectroscopy (FAB-MS), NMR spectroscopy, CV, and UV/vis spectroscopy.

[1] To whom correspondence should be addressed. Fax: (913) 537-5584. E-mail: kramer@crunch.usgmrl.ksu.edu.

[2] The Agricultural Research Service, USDA is an equal opportunity/affirmative action employer and all agency services are available without discrimination.

[3] Abbreviations used: DA, dopamine; NADA, *N*-acetyldopamine; NAcH, *N*-acetylhistidine; NAcH-NADA-I, 6-NAcH-NADA, 6-[*N*-(*N*-acetylhistidyl)]-*N*-acetyldopamine; NAcH-NADA-II, 2-NAcH-NADA, 2-[*N*-(*N*-acetylhistidyl)]-*N*-acetyldopamine; NACySH, *N*-acetylcysteine; LC, liquid chromatography; FAB-MS, fast atom bombardment mass spectrometry; NMR, nuclear magnetic resonance spectroscopy; CV, cyclic voltammetry; EC, electrochemical; DEPT, distortionless enhancement by polarization transfer; COSY-LR, long range correlated spectroscopy; TOCSY, total correlation spectroscopy; HMQC, heteronuclear multiple quantum coherence; HMBC, heteronuclear multiple-bond correlation.



0003-9861/96 $18.00

## MATERIALS AND METHODS

*Chemicals.* The following chemicals were obtained from commercial sources and used as received: NADA and NAcH (Sigma Chemical Co., St. Louis, MO)[4]; formic acid, ammonium formate, and disodium ethylenediaminetetraacetate (EDTA) (Fisher Scientific Co., Pittsburgh, PA); methanol (UV cutoff: 204 nm) (Baxter Healthcare Corporation, Burdick & Jackson Division, Muskegon, MI); KCl (Mallinckrodt Specialty Chemicals, Chesterfield, MO); and HCl (J. T. Baker Chemical Co., Phillipsburg, NJ).

*Small-scale electrochemical preparation of NADA quinone.* Small-scale preparation of NADA quinone was performed by electrolysis of 0.5 ml NADA in 0.01 M HCl and 0.09 M KCl (pH 2.0). A custom-made coulometric microcell with a platinum gauze working electrode, a Ag/AgCl (saturated KCl) reference electrode and a platinum auxiliary electrode was used. The design of the cell and the electrolysis procedure have been described in a previous paper (7). The potential for coulometric oxidation of NADA was controlled at 700 mV. Electrolyses for 2.5, 3.0, 3.5, and 4.0 min were sufficient for greater than 99% oxidation of 0.5, 1.0, 2.0, and 3.0 mM solutions of NADA, respectively. In order to perform the kinetic studies at pH 7.0, NADA quinone that is generated at pH 2.0 must be stable so that the kinetic reaction starts only at the time of mixing NADA quinone with nucleophile solution in the pH 7.0 buffer (see next section). This was demonstrated in a separate experiment, where it was observed that the decrease in absorbance at 396 nm, which is the absorption maximum of NADA quinone, was less than 0.75% over a 3 min period.

*Analytical LC, UV/vis, and electrochemical studies of the reactions of NADA quinone with NAcH.* To study compositions of a reaction mixture resulting from mixing NADA quinone and NAcH in a 1:100 molar ratio, 90 $\mu$l of 1 mM NADA quinone were mixed with 225 $\mu$l of 40 mM NAcH at pH 7.0. The pH of the mixture was 7.0. One hundred microliters of the resulting solution were analyzed by LC at 30°C. The LC system consisted of a Beckman (Berkeley, CA) model 332 gradient liquid chromatography system equipped with two model 110A pumps and a model 420 controller, a Hewlett–Packard (Palo Alto, CA) HP 8452A diode array spectrophotometer equipped with a 1-cm quartz flow cell (Pyrocell Manufacturing Co., Inc., Westwood, NJ), and a Bioanalytical Systems (West Lafayette, IN) LC-4B dual amperometric detector connected to a Hewlett–Packard HPLC ChemStation via a Hewlett–Packard 35900 multichannel interface. Separation was achieved on a Microsorb-MV C18 column (5 $\mu$m, 4.6 $\times$ 250 mm) (Rainin Instrument Co., Inc., Woburn, MA) with a binary mobile phase system in which solvents A and B were used. Solvent A was 150 mM formic acid, 30 mM ammonium formate, and 0.1 mM EDTA (pH 3.0), and solvent B was 50% methanol, 180 mM formic acid, 8 mM ammonium formate, and 0.1 mM EDTA (pH 3.0). The mobile phase gradient was 0–15 min, 80% solvent A and 20% solvent B, and 15–30 min, linear gradient from 20% solvent B to 80% solvent B; the flow rate was at 1 ml/min. UV/vis spectra of the LC effluent were recorded every 10 s for the duration of the experiment within the 220- to 550-nm wavelength range. Plots of absorbances at specific wavelengths, such as 280 nm, as a function of time are extracted from these spectral data to give desired chromatograms. The dual amperometric detector that was used for electrochemical detection of the LC effluent has a thin-layer electrochemical flow cell with two glassy carbon working electrodes, a Ag/AgCl (3 M KCl) reference electrode, and a stainless steel auxiliary electrode. The electrode potentials were 800 and −100 mV. The former potential is sufficient to oxidize NADA and the products formed from the reaction of NADA quinone and NAcH, whereas the latter potential is sufficient to reduce NADA quinone and any adduct quinone. The two working electrodes were arranged in a parallel configuration so that both electrochemically oxidizable species and reducible species in the LC effluent could be detected simultaneously. Two chromatograms were recorded from the electrochemical (EC) detector and are referred to as LC-EC (oxidation) and LC-EC (reduction) chromatograms. Since the sensitivity of electrochemical detection is much higher than that of UV/vis detection, a splitter was used between the quartz flow cell and the electrochemical flow cell in order to obtain both discernible UV spectra and within-scale electrochemical current responses for the same run. Approximately one-thirtieth of the effluent from the quartz flow cell flowed into the electrochemical flow cell.

The reactions of NADA quinone with NAcH at different molar ratios and at pH 7.0 were followed by recording UV/vis spectra in a 1.0-cm quartz cell with the HP 8452A diode array spectrophotometer. Once electrolysis of 0.5, 1.0, 2.0, or 3.0 mM NADA was complete, 0.195 ml of NADA quinone was mixed with 0.455 ml NAcH in the quartz cell at 25°C. Spectral measurement was initiated 15 s after mixing and performed for 10 min at 15-s intervals. Reaction rates were estimated from the decrease of absorption at 396 nm, which is the $\lambda_{max}$ of NADA quinone. Regression analyses of log(absorbance at 396 nm) vs time were performed to obtain the rate constants. Subtraction of the absorbance at 700 nm from the absorbance at 396 nm was used to correct for any instrument drift from one spectrum to the next. There was no absorption in the wavelength range from 700 to 800 nm.

CV of 0.3 mM NADA in the presence of 0.4 M NAcH at pH 7.0 was performed using a Bioanalytical Systems BAS-100W electrochemical system. A BAS glassy carbon electrode with an area of 7.1 $mm^2$ was used as the working electrode. The reference and auxiliary electrodes were a Ag/AgCl (saturated KCl) electrode and a platinum wire electrode, respectively. A small electrochemical cell with a capacity of 1 ml was used. The scan rates varied from 50 to 200 mV/s.

*Synthesis and purification of products from reactions of NADA quinone with NAcH.* To synthesize relatively large amounts of products from reactions of NADA quinone with NAcH, a custom-made flow-through coulometric cell designed for larger scale oxidations was used (X. Huang *et al.*, unpublished data). A solution of NADA in 0.01 M HCl and 0.09 M KCl was passed through the cell and oxidized. The NADA quinone effluent was then added dropwise into a stirred NAcH solution at pH 7.0. After the reaction mixture was lyophilized to reduce the volume, the resulting solution was subsequently filtered and subjected to semipreparative LC separation. The LC system described above was used, but with the electrochemical detector disconnected. Separation was achieved on a Phenomenex (Torrance, CA) C18 semipreparative column (10 $\mu$m, 250 $\times$ 10 mm). The gradient employed was 0–25 min, 90% solvent A and 10% solvent B, and 25–35 min, linear gradient from 10% solvent B to 80% solvent B. The flow rate was 4 ml/min. Each product fraction was collected and subjected to a desalting step using the semipreparative LC column. After a product solution was injected onto the column, the salt components were eluted using distilled water as the mobile phase. The product was subsequently eluted using 25% methanol and then lyophilized to dryness.

*Characterization of products.* FAB-MS was performed on a Hewlett–Packard HP 5989A MS Engine. The following NMR experiments were carried out either with a Varian (Palo Alto, CA) UNITY*plus* 400 MHz spectrometer at 27°C or with a Varian UNITY*plus* 500 MHz spectrometer at 30°C: proton, carbon-13, distortionless enhancement by polarization transfer (DEPT) (8), long range $^1H$-$^1H$ correlated spectroscopy (COSY-LR) (9), total correlation spectroscopy (TOCSY) (10), heteronuclear multiple quantum coherence correlation (HMQC) (11), and heteronuclear multiple-bond correlation (HMBC) (12) NMR experiments. Products were dissolved in 0.8 ml of either $D_2O$ or $H_2O$:$D_2O$ (90:10). On one occasion, a product was dissolved in 0.83 ml acetone-$d_6$:$D_2O$ (80:3) in order to resolve the aromatic $^1H$ resonances. UV/vis spectroscopic measurements of the reaction products in 0.01 M HCl were conducted using the HP 8452A diode-array spectrophotometer with a 1.0-cm quartz cuvette. Cyclic

[4] Mention of a proprietary product does not constitute a recommendation by the USDA.

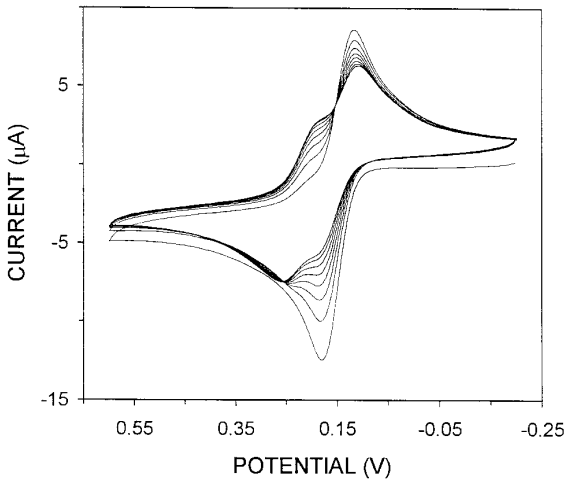


FIG. 1. Cyclic voltammogram of 0.3 mM NADA in 0.4 M NAcH solution (pH 7.0). The scan was initiated in the positive-going direction from −0.2 V at a rate of 50 mV/s.

voltammograms of NADA and reaction products in 0.1 M potassium phosphate buffer (pH 7.0) were obtained using the BAS-100W electrochemical system (scan rate: 200 mV/s).

## RESULTS

### *Studies of the Reactions of NADA Quinone with NAcH*

*Cyclic voltammetry.* The electrochemical behavior of NADA in the presence of NAcH at pH 7.0 was studied using cyclic voltammetry. A voltammogram obtained at a scan rate of 50 mV/s is shown in Fig. 1. In the first cycle, the voltammogram of NADA consists of a single anodic peak at 0.18 V for the two-electron oxidation of NADA to NADA quinone and a corresponding cathodic peak at 0.12 V for the reduction of NADA quinone to starting material. In subsequent cycles, another redox couple appears at a potential that is 80 mV more positive than that for the NADA/NADA quinone couple. As the scan number increases or as the scan rate decreases, the magnitudes of the peaks for this new couple increase at the expense of the peaks for the NADA/NADA quinone couple. Since the new redox couple is not formed when NAcH is absent, these results indicate that NADA quinone undergoes a relatively slow chemical reaction with NAcH under these conditions to give one or more products that are oxidized at more positive potentials.

*UV/vis spectroscopy.* The kinetic behavior of NADA quinone in NAcH solutions was studied spectroscopically under pseudo first-order conditions, i.e., the analytical concentration of NAcH was at least ten times greater than that of the quinone. The spectral changes that are associated with the reaction of 0.3 mM NADA quinone with 50 mM NAcH at pH 7.0 are shown in Fig.

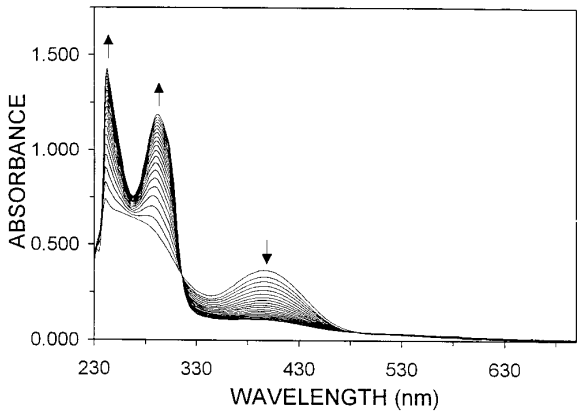


FIG. 2. Spectral change associated with the reactions of 0.3 mM NADA quinone with 50 mM NAcH at pH 7.0. Spectral measurements were conducted at 15-s intervals from 15 to 600 s after mixing of the two solutions. Only every other spectrum is shown.

2. The absorbance at the $\lambda_{max}$ of the quinone, 396 nm, decreases with time, whereas absorbances at 242 and 284 nm increase, indicating that consumption of the quinone and formation of a new product(s) occur.

Rate constants for the reaction of NADA quinone with NAcH were estimated on basis of the rate of decrease in NADA quinone's absorbance at 396 nm. The dependence of the rate constant for the reaction of NADA quinone on quinone concentration was studied using solutions of 0.15, 0.3, 0.6, and 0.9 mM NADA quinone in 200 mM NAcH at pH 7.0. As expected for a pseudo-first-order reaction, the rate constant for the NADA quinone reaction is independent of quinone concentration (data not shown). The dependence of the reaction rate on NAcH was also studied using 0.3 mM NADA quinone with 20, 50, 100, and 200 mM NAcH. The results demonstrate that the pseudo-first-order rate constant exhibits a linear dependence on the concentration of NAcH (Fig. 3). For 0.3 mM NADA quinone

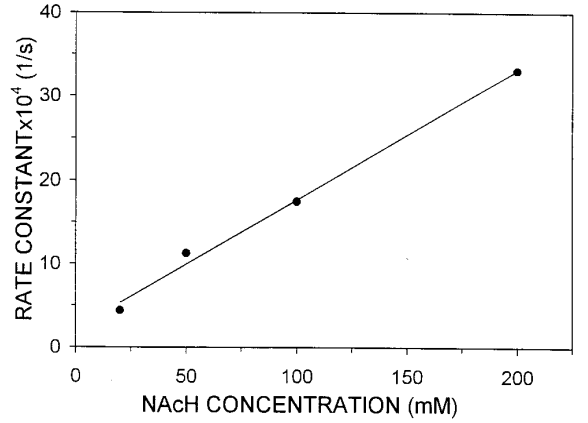


FIG. 3. Pseudo-first-order rate constants of reactions of NADA quinone with NAcH at pH 7.0 as a function of NAcH concentration.

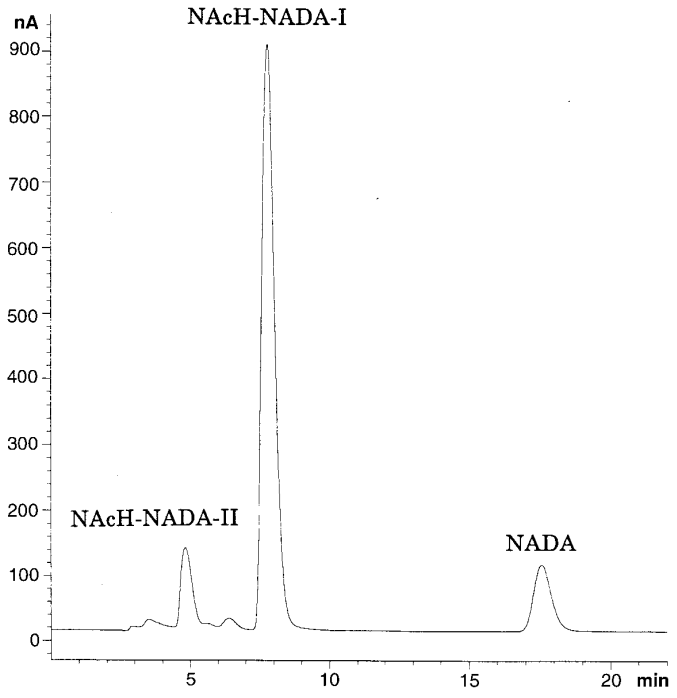


FIG. 4. LC-EC (oxidation) of the reaction mixture of NADA quinone with NAcH. Mobile phase: 0–15 min, 20% B; 15–30 min, linear gradient from 20 to 80% B. Flow rate, 1 ml/min.

in 100 mM NAcH solution, values of $1.8 \times 10^{-3}$ $s^{-1}$ and $1.8 \times 10^{-2}$ $M^{-1}s^{-1}$ were calculated for the pseudo-first-order and second-order rate constants, respectively. The positive intercept is due to inherent slow reactions of NADA quinone with unidentified components of the solvent electrolyte buffer system.

*Analytical LC.* A 100-$\mu$l aliquot of the solution obtained from mixing 90 $\mu$l of 1 mM NADA quinone with 225 $\mu$l of 40 mM NAcH at pH 7.0 was analyzed by LC. There were no discernible peaks in the LC-EC (reduction) chromatogram, which indicates that the quinone had been consumed quantitatively. The LC-EC (oxidation) chromatogram is shown in Fig. 4. The principal product, NAcH-NADA-I, eluted at 7.8 min, while the second most prominent product, NAcH-NADA-II, eluted at 4.8 min. A minor unidentified product eluted at 6.2 min. The peak at 17.4 min is due to NADA.

Another chromatogram displaying absorbance at 280 nm as a function of elution time was extracted from UV/vis spectra of the LC effluent of the reaction mixture at pH 7.0 (data not shown). The relative yields of the two major products were estimated on the basis of their 280-nm chromatographic peak areas, assuming equal molar absorption coefficients for the two products (*vide infra*). The relative molar ratio of NAcH-NADA-I to NAcH-NADA-II is approximately 87:13. Semipreparative LC was performed to purify the two major products, which were white powders after lyophilization.

*NMR and MS Analyses of the Reaction Products*

The purified reaction products NAcH-NADA-I and NAcH-NADA-II were characterized by FAB-MS. Both products have $MH^+$ at m/z = 391 (spectra not shown). These results indicate that each of the products is a mono-addition adduct of NAcH with NADA quinone (theoretical m/z = 391).

The structure of the NAcH-NADA-I adduct was elucidated by 1D-$^1$H and $^{13}$C NMR experiments, and 2D-$^{13}$C-$^1$H HMQC and $^1$H-$^1$H TOCSY NMR experiments (Fig. 5). The chemical shift assignments are summarized in Table I. The $^1$H resonance signal at 8.80 ppm is assigned to H2′ according to a NAcH spectrum previously reported in the literature (13). The doublet at 8.30 ppm is assigned to NH8′ that is next to a CH and resonates at a lower field than aromatic protons. The broad peak at 7.85 ppm is assigned to NH9 that resonates at a lower field than any of the aromatic protons. NH8′ at 8.30 ppm shows cross peaks at 3.35 and 3.15 ppm, respectively, in the $^1$H-$^1$H TOCSY spectrum, which indicates that one of the C(6′) protons, H6′a, resonates at 3.35 ppm, and the other, H6′b, gives rise to the resonance at 3.15 ppm. The $^{13}$C-$^1$H HMQC spectrum also confirms that the resonance of C6′ (26 ppm) is connected to the $^1$H resonances at 3.35 and 3.15 ppm. The $^1$H resonance of NH9 shows connectivities to those at 3.15 and 2.50 ppm in the $^1$H-$^1$H TOCSY spectrum. This result, along with the fact that the —$CH_2$— resonances are shifted more to a lower field when they are proximal to an NH group than when they are next to a benzene ring, indicates that the chemical shifts at 3.15 and 2.50 ppm are due to H8 and H7, respectively. The aromatic region shows two singlets in the $^1$H spectrum as well as three proton and three carbon resonances in the HMQC spectrum. The $^1$H resonance at 7.40 ppm shows connectivity to that of H2′ at 8.80 ppm in TOCSY, which demonstrates that the peak at 7.40 ppm is due to H5′. The $^1$H resonance signals at 6.90 ppm are due to two protons on the benzene ring. They are overlapped in the $^1$H spectrum, but are more resolved in the HMQC spectrum. In order to further assign these two protons, an $^1$H experiment was conducted in an alternative solvent containing 0.80 ml acetone-$d_6$ and 0.03 ml $D_2O$. The two protons exhibited two well-resolved singlets (6.90 and 6.92 ppm) in the $^1$H spectrum obtained in the mixed acetone-$d_6$/$D_2O$ solvent (data not shown). Since neither *o*-coupling nor *m*-coupling patterns are observed, the resonances of 6.90 ppm in $H_2O$/$D_2O$ are assigned to H2 and H5. The H7′ resonance was obscured in spectra obtained from sample dissolved in $H_2O$, but did appear in spectra acquired in $D_2O$ at 4.4 ppm (data not shown). Therefore, NAcH-NADA-I is a 6-addition adduct, 6-[*N*-(*N*-acetylhistidyl)]-*N*-acetyldopamine (Scheme I).

The structure of NAcH-NADA-II adduct was also

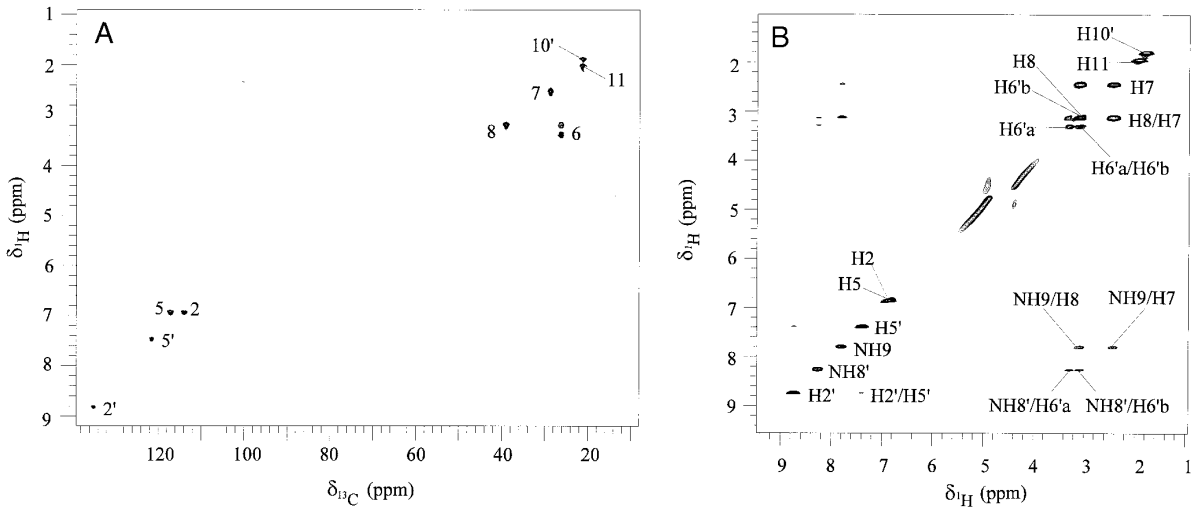


FIG. 5. 2D NMR spectra of NAcH-NADA-I obtained from the reaction of NADA quinone with NAcH. (A) $^{13}C$-$^1H$ HMQC NMR spectrum ($D_2O$); (B) $^1H$-$^1H$ TOCSY NMR spectrum [$H_2O$:$D_2O$ (85:15)]. The strong peaks near 5 ppm are due to HOD.

elucidated by 1D-$^1H$, $^{13}C$, DEPT NMR experiments, and 2D $^{13}C$-$^1H$ HMQC, HMBC NMR experiments (Fig. 6). These results are summarized in Table II. Several proton resonance peaks in the $^1H$ and $^{13}C$-$^1H$ HMQC spectra of this adduct are present in pairs, which may be due to a slow conformational change in the structure over the NMR time scale. Since the $^1H$ spectrum is quite complex, HMQC and HMBC spectra were used to assign the structure (Figs. 6A and 6B). Three C-H connectivities are present in the aromatic region of the HMQC spectrum, one of which must be due to C-H at the 5′ position of the imidazole ring and two of which must be due to two of the C-H's at the 2, 5, and 6 positions of the benzene ring. Since the resonance signals do not overlap in this region, the NAcH group must be attached to the aromatic ring.

$^{13}C$ and DEPT experiments were conducted to confirm that the *N*-acetylhistidyl moiety is not attached to the NADA side chain aliphatic carbons. The DEPT spectrum exhibits three 180° out-of-phased signals, demonstrating that three -$CH_2$- groups are present in the molecule, one of which is in the *N*-acetylhistidyl moiety and two in the NADA side chain (data not shown). These results confirm that the NAcH moiety is bound to the NADA aromatic ring.

The position of the NADA ring to which the *N*-acetylhistidyl moiety is attached in NAcH-NADA-II was assigned as follows. In the HMBC spectrum, H8 at 3.15 and 3.38 ppm exhibits connectivity with the

TABLE I

Chemical Shift Assignments and Connectivities Provided by the 2D NMR Experiments for NAcH-NADA-I

| Proton NMR | | $^1H$ | HMQC | TOCSY connectivity | |
|---|---|---|---|---|---|
| $\delta$, ppm | Peak types[a] | assignment | connectivity | $\delta$, ppm | proton |
| 8.80 | s | H2′ | 135 | 7.40 | H5′ |
| 8.30 | d | NH8′ | — | 3.35, 3.15 | H6′a, H6′b |
| 7.85 | m | NH9 | — | 3.15′, 2.50 | H8, H7 |
| 7.40 | s | H5′ | 122 | 8.80 | H2′ |
| 6.90 | s | H2, H5 | 117/114 | — | — |
| 3.35 | dd | H6′a | 26 | 8.30, 3.15 | NH8′, H6′b |
| 3.15 | m | H6′b | 26 | 8.30, 3.35 | NH8′, H6′a |
| 3.15′ | m | H8 | 39 | 7.85, 2.50 | NH9, H7 |
| 2.50 | m | H7 | 29 | 7.85, 3.15 | NH9, H8 |
| 2.00 | s | H11 | 22 | — | — |
| 1.85 | s | H10′ | 22 | — | — |

[a] s, singlet; d, doublet; m, multiplet; dd, doublet of doublet.

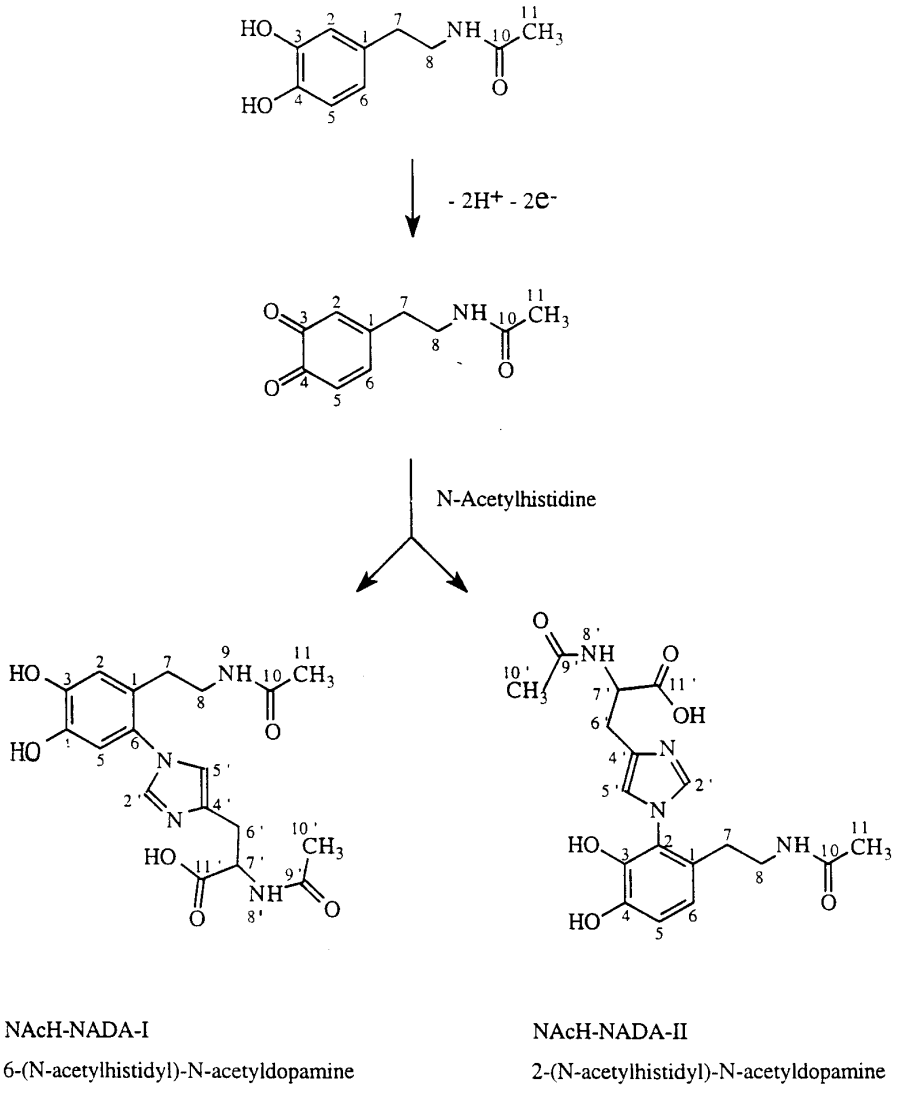


NAcH-NADA-I
6-(N-acetylhistidyl)-N-acetyldopamine

NAcH-NADA-II
2-(N-acetylhistidyl)-N-acetyldopamine

SCHEME I

carbon resonance at 129 ppm, which must be due to C1. The H7 proton at 2.35 and 2.56 ppm exhibits three connectivities with aromatic carbon signals at 129, 124, and 115 ppm. Therefore, resonances at 124 and 115 ppm are due to C2 and C6, respectively. Moreover, C7 at 29 ppm exhibits connectivity with one rather than two aromatic protons. Since NAcH-NADA-I has already been identified as the C6 addition adduct, the proton at 7.02–7.04 ppm must be due to H6 and the *N*-acetylhistidyl moiety must be attached to C2. This conclusion is corroborated by the fact that H6 shows connectivity with C2 at 124 ppm in the HMBC spectrum, whereas C2 exhibits no connectivity with any proton in the HMQC spectrum. The COSY-LR spectrum is consistent with this assignment (data not shown). Therefore, NAcH-NADA-II is identified as the 2-addition adduct, 2-[*N*-(*N*-acetylhistidyl)]-*N*-acetyldopamine (Scheme I).

### *UV/vis and Electrochemical Characterization of the Reaction Products*

The two principal reaction products were also characterized using UV/vis spectroscopy and cyclic voltammetry (data not shown). The UV/vis spectra show that both adducts have the same $\lambda_{max}$ value at 284 nm, whereas CV data demonstrate that both adducts are more difficult to oxidize than NADA. The data from the characterization of these adducts are summarized in Table III.

## DISCUSSION

Two major products were obtained from the reactions of NADA quinone with NAcH at pH 7.0 (Scheme I).

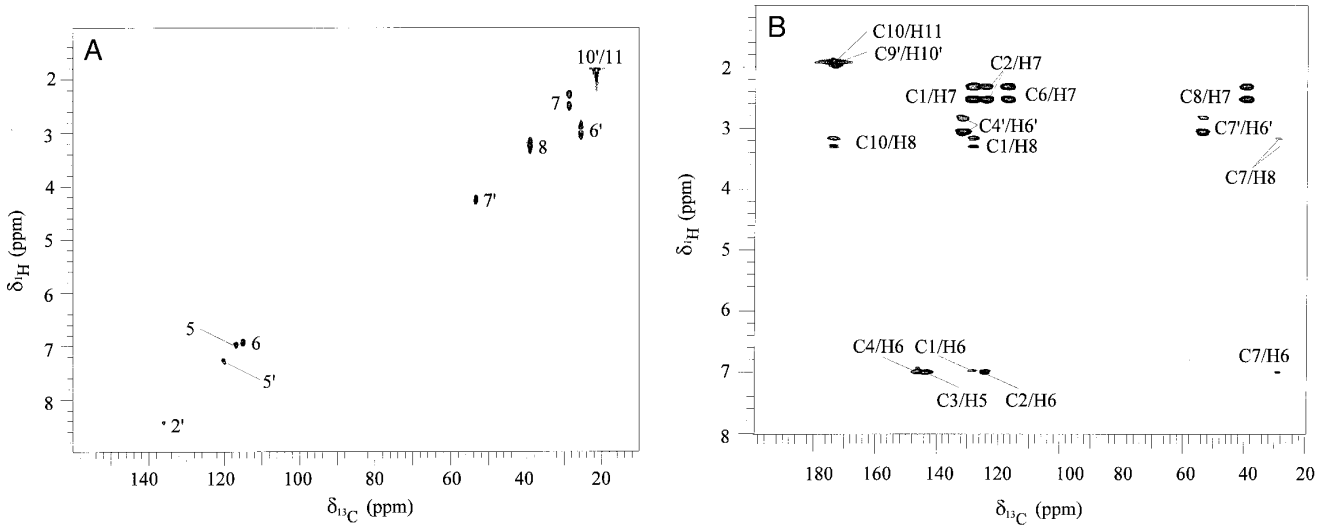


FIG. 6. 2D NMR spectra ($D_2O$) of NAcH-NADA-II obtained from the reaction of NADA quinone with NAcH. (A) $^{13}C$-$^1H$ HMQC NMR spectrum; (B) $^{13}C$-$^1H$ HMBC NMR spectrum.

The most abundant product is 6-NAcH-NADA, which is the Michael 1,4-addition adduct of NADA quinone at C6 of the ring. The second major product is 2-NAcH-NADA, the Michael 1,6-addition adduct of NADA quinone at C2 of the ring. The detection of 6-NAcH-NADA is consistent with a previous study where NADA was mixed with NAcH in the presence of insect cuticle dissected from late fifth instar larvae of *H. cecropia* (2). In that study, the 2-NAcH-NADA adduct was not detected in the cuticle-catalyzed coupling study (2). However, because C2 is more sterically hindered, which is consistent with its NMR peak splitting, the 2-adduct might not be produced to a significant extent under the conditions used (2). In the NADA-NAcH-cuticle system, a $\beta$-side chain adduct was detected, which the authors suggested arose from the *p*-quinone methide intermediate (2). However, no side-chain addition adduct was detected in our system. The results indicated that (1) spontaneous tautomerization of *o*-quinone to *p*-quinone methide does not occur under our conditions and (2) an enzyme, quinone–quinone methide isomerase, would be needed to convert the quinone to its quinone methide isomer for $\beta$-carbon addition if it were to occur.

TABLE II

Chemical Shift Assignments and Connectivities Provided by the 2D NMR Experiments for NAcH-NADA-II

| Proton NMR $\delta$, ppm | $^1H$ assignment | HMQC connectivity $\delta$, ppm | HMBC connectivity | |
|---|---|---|---|---|
| | | | $\delta$, ppm | carbon |
| 8.50 | H2′ | 136 | — | — |
| 7.38, 7.32 | H5′ | 120 | 136, 132 | C2′, C4′ |
| 7.06 | H5 | 117 | 143 | C3 |
| 7.04, 7.02 | H6 | 115 | 144, 129, 124, 29 | C4, C1, C2, C7 |
| 4.34, 4.28 | H7′ | 54 | — | — |
| 3.38, 3.15 | H8 | 39 | 174, 129, 29 | C10, C1, C7 |
| 3.06, 2.82 | H6′ | 26 | 132, 54 | C4′, C7′ |
| 2.56, 2.35 | H7 | 29 | 129, 124, 115, 39 | C1, C2, C6, C8 |
| 1.92 | H11/H10′ | 22 | 174 | C10/C9′ |

It is worthwhile to compare this system with a previously investigated system in which reactions of dopamine (DA) quinone with another protein model nucleophile, *N*-acetylcysteine (NACySH), yielded C2 and C5 mono-addition adducts as well as a C2, C5 di-addition adduct (14). First, no di-addition adducts were identified in the current system. This result is consistent with the observation that the mono-addition *N*-acetylhistidyl adducts are oxidized at 80 to 100 mV more positive potentials than NADA, which means that formation of a di-NAcH-adduct is not favored under our reaction conditions. Presumably, if electrolysis were performed continuously, or if oxidation were carried out either enzymatically or with an excess of chemical oxidant, then the mono-NAcH-NADA adducts would be oxidized and a di-addition adduct subsequently would be produced. In contrast, mono-addition *N*-acetylcysteinyl adducts of DA quinone are oxidized more readily than DA (14). This results in oxidation of the mono-addition adduct by unreacted DA quinone, which causes the mono-addition adduct quinone and DA to be formed. This mono-addition adduct quinone then reacts with the NACySH nucleophile that is present in large excess to form the di-adduct, 2,5-di-NACyS-DA. Second, the principal nucleophilic attacks occur at dif-

TABLE III

Characteristic Data of NADA and Its NAcH Adducts

| Compound[a] | MW[b] | R.T. (min)[c] | Rel. yield[d] | UV: $\lambda_{max}$ ($\log\epsilon$)[e] | CV: $E_{pa}$, $E_{pc}$ (mV)[f] |
|---|---|---|---|---|---|
| NADA | 195 | 17.4 | na | 280 (3.38) | 220, 95 |
| 6-NAcH-NADA | 390 | 7.8 | 87% | 284 | 300, 170 |
| 2-NAcH-NADA | 390 | 4.8 | 13% | 284 (3.46) | 340, 170 |

[a] See Scheme I for structures of the adducts.

[b] The molecular weights were determined using FAB-MS.

[c] Retention times were obtained from the LC-EC chromatogram of the reaction mixture at pH 7.0 (Fig. 4).

[d] The relative yields of the two major products were estimated based on their peak areas in the LC-UV/vis chromatogram (not shown) of the reaction mixture at pH 7.0 (assuming comparable molar absorption coefficients).

[e] UV/vis spectra of products were obtained during LC analysis. Molar absorption coefficients were obtained in 0.01 M HCl. The molar absorption coefficient of 6-NAcH-NADA was not measured.

[f] Cyclic voltammetric data were obtained on a 7.1-$mm^2$ glassy carbon electrode at a scan rate 200 mV/s in 0.1 M phosphate buffer at pH 7.0.

ferent positions of the ring in these systems. The actual cause of the regioselectivity is unclear, although several hypotheses have been proposed (15, 16). Third, the reaction of DA quinone with NACySH is at least $10^6$ times faster than the reaction of NADA quinone with NAcH, which is based on the estimate of the second order rate constants of these systems at neutral pH (14). Fourth, C2-addition adducts are formed in both systems, which indicates that C2 of the ring in both DA and NADA quinone is readily accessible to both nucleophiles.

It has been proposed in the literature that catecholamine quinones can cross-link two cuticular protein molecules either via C6 of the aromatic ring and the $\beta$-carbon (C7) (1) or via $\alpha$- (C8) and $\beta$-carbons (3). However, the fact that both C2 and C6 of the NADA quinone ring undergo nucleophilic attack and that no attack occurs at the $\beta$-carbon suggests the possibility of C2 and C6 of the NADA ring moiety being the primary sites where the cross-linking takes place, resulting in sclerotization of insect cuticle.

Protein-bound catecholamines were detected previously in rat neostriatal tissue slices incubated with $^3$H-dopamine (17). Acid hydrolysis of the protein extract revealed the presence of radiolabeled cysteinyldopamine and cysteinyl-dihydroxyphenylacetic acid residues, suggesting that dopamine oxidizes to form a reactive metabolite, presumably a quinone, which then reacts with nucleophilic sulfhydryl groups of cysteinyl residues in the proteins. Tyrosinase-catalyzed binding of DOPA with several proteins, including bovine serum albumin, through the sulfhydryl group and perhaps other nucleophilic side chains *in vitro* has also been demonstrated (18). A similar type of mechanism occurs in insect cuticle during sclerotization and catecholamine-containing proteins have been extracted from cuticle (6). However, the residues in the cuticular proteins that act as nucleophiles for the quinones have not been directly identified (1). Because the occurrence of cysteine in cuticular proteins is rare, histidyl and lysyl residues are apparently more likely to be nucleophiles and, indeed, those residues have been implicated by solid state NMR evidence (4, 5). Results obtained from this study provide additional evidence supporting the hypothesis that histidyl residues in the cuticular proteins serve as the primary group of nucleophiles for quinonoid intermediates during cuticle sclerotization.

## ACKNOWLEDGMENTS

The authors thank Dr. B. Plashko for performing FAB-MS experiments and Dr. M. Collinson for providing the BAS-100W electrochemical system. We are grateful to Dr. T. L. Hopkins for assistance with this study and for reviewing the manuscript. We also thank Dr. G. Dryhurst (University of Oklahoma) and Dr. D. Hua (Kansas State University) for reviewing an earlier draft of the manuscript. This research was supported in part by National Science Foundation Grants DCB-9019400, MCB-9418129, and CHE-9216101 and was a cooperative investigation between the Agricultural Research Service and the Kansas Agricultural Experimental Station (Contribution No. 96-154-J).

## REFERENCES

1. Hopkins, T. L., and Kramer, K. J. (1992) *Annu. Rev. Entomol.* 37, 273–302.
2. Andersen, S. O., Peter, M. G., and Roepstorff, P. (1992) *Insect Biochem. Mol. Biol.* 22, 459–469.
3. Ricketts, D., and Sugumaran, M. (1994) *J. Biol. Chem.* 269, 22217–22221.
4. Schaefer, J., Kramer, K. J., Garbow, J. R., Jacob, G. S., Stejskal, E. O., Hopkins, T. L., and Speirs, R. D. (1987) *Science* 235, 1200–1204.
5. Christensen, A. M., Schaefer, J., Kramer, K. J., Morgan, T. D., and Hopkins, T. L. (1991) *J. Am. Chem. Soc.* 113, 6799–6802.

6. Okot-Kotber, B. M., Morgan, T. M., Hopkins, T. L., and Kramer, K. J. (1994) *Insect Biochem. Mol. Biol.* 24, 787–802.
7. Xu, R., Huang, X., Kramer, K. J., and Hawley, M. D. (1995) *Anal. Biochem.* 231, 72–81.
8. Bendall, M. R., and Pegg, D. T. (1983) *J. Magn. Reson.* 53, 272–296.
9. Bolton, P. H., and Bodenhauser, G. (1982) *Chem. Phys. Lett.* 89, 139–144.
10. Braunschweiler, L., and Ernst, R. R. (1983) *J. Magn. Reson.* 53, 521–528.
11. Marion, D., Ikura, M., Tschudin, R., and Bax, A. (1989) *J. Magn. Reson.* 85, 393–399.
12. Bax, A., and Summers, M. F. (1986) *J. Am. Chem. Soc.* 108, 2093–2094.
13. Sasaki, S. (1985) Handbook of Proton-NMR Spectra and Data. Vol. 7. Academic Press, Orlando.
14. Xu, R., Huang, X., Kramer, K. J., and Hawley, M. D. (1996) *Bioorg. Chem.*, in press.
15. Chavdarian, C. G., and Castagnoli, N., Jr. (1979) *J. Med. Chem.* 22, 1317–1322.
16. Sugumaran, M., Dali, H., and Semensi, V. (1989) *Arch. Insect Biochem. Physiol.* 11, 127–137.
17. Hasting, T. G., and Zigmond, M. J. (1994) *J. Neurochem.* 63, 1126–1132.
18. Kato, T., Ito, S., and Fujita, K. (1986) *Biochim. Biophys. Acta* 881, 415–421.